AD-A084 430 CORNELL UNIV ITHACA NY DEPT OF THEORETICAL AND APPL--ETC F/G 21/2
MATHEMATICAL THEORY OF LAMINAR COMBUSTION. VI. SPHERICAL DIFFUS--ETC(U)
MAR 80 J D BUCKMASTER, G S LUDFORD DAAG29-79-C-0121
UNCLASSIFIED TR-108 ARO -15882.17-M NL

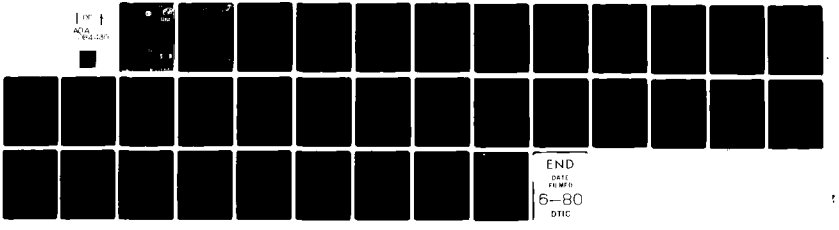

END
DATE FILMED
6-80
DTIC

LEVEL II

12

(6) MATHEMATICAL THEORY OF LAMINAR COMBUSTION, VI.

Spherical Diffusion Flames

(9) (14) TR-

Technical Report No. 108

(10) J.D. Buckmaster & G.S.S. Ludford

(11) March 1980

(12) 35

(18) HKO

(19) 15882.17-M

U.S. Army Research Office
Research Triangle Park, NC 27709

(15) Contract No. DAAG29-79-C-0121

Cornell University
Ithaca, NY 14853

Approved for public release; distribution unlimited

Forward

This report is Chapter VI of the twelve in a forthcoming research monograph on the mathematical theory of laminar combustion. Chapters I-IV originally appeared as Technical Reports Nos. 77, 80, 82 & 85; these were later extensively revised and then issued as Technical Summary Reports No's 1803, 1818, 1819 & 1888 of the Mathematics Research Center, University of Wisconsin, Madison. References to I-IV mean the MRC reports.

Contents

The findings in this report are not to be construed as an official Department of the Army position unless so designated by other authorized documents.

Chapter VI
Spherical Diffusion Flames

1. Introduction

Earlier chapters have been concerned with flames for which the reactants are supplied already mixed. When the reactants are intially separated and diffuse into each other to form a combustible mixture, the flame is called a diffusion flame. A bunsen burner with its air hole closed supports a diffusion flame between the gas supplied through the tube and the surrounding oxygen-rich atmosphere. A candle supports a vapor diffusion flame, so-called because the fuel is produced, through liquefaction and subsequent evaporation of the wax, by the heat of the flame itself.

Premixed and diffusion flames share certain features, but the differences are more striking than the similarities. For example, there is no unlimited plane flame, as can be seen from Sec. II.7. The oxidant fraction would be constant beyond the flame sheet, at which the value would be smaller than upstream. But a diffusion flame requires the oxidant fraction to be zero upstream, since otherwise there is premixing, so that a contradiction is reached. A similar argument applies when the fuel is supplied at a finite point, where now it is the oxidant flux which must be zero. Moreover, since cylindrical flames are just geometrically attenuated versions of plane flames (Ch. VII), there is no cylindrical diffusion flame either (Ludford 1977).

In order to gain some insight into the nature of diffusion flames we seek a simple one-dimensional configuration which bears some relation to physical reality. One possibility is to introduce the oxidant at a finite point of the plane flame but, curiously enough, details of that have never been worked out. To be sure, the chambered diffusion flame, in which the fuel supply is also at a finite point, has recently been considered by Matalon, Ludford and Buckmaster

(1978). But that is already too complicated for our purposes.

Two choices have been popular in the literature. One is the counterflow diffusion flame (Fig. 1) in which opposing jets of fuel and oxidant collide, supporting a locally one-dimensional flame in the neighborhood of the stagnation point. The configuration has the advantage of being relatively easy to set up experimentally but suffers analytically from the gross compromises which have to be made with the fluid mechanics. For that reason, and because of its similarity with the alternative to be discussed next, we shall not consider the counterflow diffusion flame.

The second choice is the spherical diffusion flame which, because it occurs in the burning of fuel drops (Fig. 2), has great technological interest. As for the candle, it is then a vapor flame, the liquid fuel being vaporized at its assumed spherical surface by heat conducted back from the surrounding flame where the vapor burns with the ambient oxidant. Although the size of the drop continually decreases as fuel is consumed, the quasi-steady approximation (Williams, 1965) neglects this effect. Such steady burning can be produced experimentally by forcing the fuel through a porous sphere in a gravity-free environment. Indeed, by supplying the fuel already as a vapor the whole range of spherical flames can be examined.

If these phenomena are studied for the express purpose of solving the practical problem from which they derive, then one has to be concerned with the validity of the modelling. Thus many studies of the fuel-drop problem have examined amongst other things the validity of the quasi-steady approximation, about which reservations have been expressed. Such practical considerations are not our concern, since we regard the models simply as mathematical idealizations, albeit with physical reality continually in mind, whose study can provide some insight into the nature of diffusion flames. The experimentalist may then feel

challenged to devise real flames which model the mathematics, as in the porous-sphere experiment mentioned above.

We have to deal with the spherically symmetric form of the equations (I.41-44), in particular

$$(1) \qquad \frac{1}{\theta}\frac{\partial \rho}{\partial \tau} + \frac{1}{r^2}\frac{\partial}{\partial r}(r^2 \rho v) = 0 \ ,$$

$$(2) \qquad \rho\left(\frac{1}{\theta}\frac{\partial T}{\partial \tau} + v\frac{\partial T}{\partial r}\right) - \frac{1}{r^2}\frac{\partial}{\partial r}\left(r^2 \frac{\partial T}{\partial r}\right) = \Omega \ ,$$

$$(3) \qquad \rho\left(\frac{1}{\theta}\frac{\partial Y_i}{\partial \tau} + v\frac{\partial Y_i}{\partial r}\right) - \frac{1}{\mathcal{L}_i}\cdot\frac{1}{r^2}\frac{\partial}{\partial r}\left(r^2\frac{\partial Y_i}{\partial r}\right) = \alpha_i \Omega \qquad (i = 1,2),$$

where the radial velocity v is the only component, $T = 1/\rho$, $\tau = t/\theta$ and (if the radius, a, of the supply sphere is used to define units)

$$(4) \qquad \Omega = D\, Y_1^{\nu_1} Y_2^{\nu_2}\, e^{-\theta/T}$$

with D given by the formula (I.47). The equations for the product and inert species, which have not been written, are complicated by the implicit assumption that $\mathcal{L}_1$ is not necessarily equal to $\mathcal{L}_2$. The momentum equation, which has also been omitted, plays no role other than determining the pressure field when there is spherical symmetry. Throughout this chapter we shall take

$$(5) \qquad \nu_1 = \nu_2 = 1 \quad \text{so that} \quad \alpha_1 = \alpha_2 = -\tfrac{1}{2}$$

(corresponding to a bimolecular reaction) for the sake of simplicity, even though retaining general values would cover the corresponding analysis in Ch. VII ($\nu_1 = 1$, $\nu_2 = 0$) showing, in particular, why there are so many similarities. Finally, unsteady terms have been retained with a view to stability considerations

on the long time τ. To avoid subscripts we shall change the notation to

$$(6) \qquad Y_1 = Y,\ Y_2 = Z,\ J_1 = J,\ J_2 = K,\ \mathcal{L}_1 = \mathcal{L},\ \mathcal{L}_2 = \mathcal{M} .$$

All six values T_s, Y_s, Z_s, T'_s, Y'_s, Z'_s may be assigned at the supply sphere. In varying the mass flux M from the sphere we shall in fact suppose that $M^{-1}T'_s$, $M^{-1}Y'_s$, $M^{-1}Z'_s$ are prescribed, these being fluxes per unit mass of mixture supplied. (The same was true for the plane flame; M was then hidden in the coordinate.) It is more convenient to suppose that the two fluxes

$$(7) \qquad J_s = Y_s - M^{-1}Y'_s/\mathcal{L} \ , \ K_s = Z_s - M^{-1}Z'_s/\mathcal{M}$$

are given. Clearly a pure diffusion flame requires $J_s > 0$, $K_s = 0$ so that the sphere is a source of fuel but not of oxidant; for simplicity again, we shall take

$$(8) \qquad J_s = 1,\ K_s = 0$$

making the sphere purely a source of fuel. Likewise the values T_∞, Z_∞ at infinity will be given, leaving only $T_s, M^{-1}T'_s = L$ among the six original parameters.

In addition Y_∞ may be assigned, and we shall take

$$(9) \qquad Y_\infty = 0$$

to ensure that all the fuel has originated at the supply. There are then seven boundary conditions on the sixth-order system, so that we may expect M to be determined by D.

2. Steady Combustion for $\mathcal{L} = \mathcal{M} = 1$. Damköhler Number Asymptotics.

The qualitative nature of the steady solution is not affected by the Lewis numbers; it is only in the stability question that they play an important role.

To simplify the discussion, which will be complicated enough, we shall therefore assume for the present that both Lewis numbers are unity.

In the steady state the continuity equation can be integrated to give

$$r^2 \rho v = M \text{ (const.)} \quad \text{or} \quad \rho v = M/r^2. \tag{10}$$

$4\pi a^2 M$ is the rate at which fuel is supplied, but is is only the burning rate if the total outflow of fuel at infinity is zero. Nevertheless M is loosely called the burning rate, and we shall adopt the term also.

The Shvab-Zeldovich variables $\tilde{Y}_i = T - Y_i/\alpha_i$ satisfy

$$\mathcal{D}(\tilde{Y}_i) \equiv \left[\frac{1}{r^2}\frac{d}{dr}\left(r^2 \frac{d}{dr}\right) - \frac{M}{r^2}\frac{d}{dr}\right]\tilde{Y}_i = 0 \quad \text{for} \quad 1 < r < \infty . \tag{11}$$

Since all solutions are bounded at infinity, the analysis immediately differs from that for the plane (premixed) flame. As already anticipated, all six basic parameters T_0, L, J_0, K_0, T_∞, $Y_{0\infty}$, Z_∞ may be assigned to give, in the case (8)

$$T+2Y = T_\infty + (T_a - T_\infty)(1-e^{-M/r}), \tag{12}$$

$$T+2Z = (T_s - L)(1-e^{-M/r}) + (T_\infty + 2Y_{0\infty} - Z_\infty)e^{-M/r} \tag{13}$$

where

$$T_a = T_s - L + 2 \tag{14}$$

is the adiabatic flame temperature. The problem now reduces to one for T alone, namely

$$\mathcal{D}(T) = DYZ\, e^{-\theta/T} \quad \text{for} \quad 1 < r < \infty , \tag{15}$$

T_s, L, T_∞ prescribed.

Since there are three boundary conditions for this second-order differential equation, M is determined as a function of D as part of the solution.

Until the advent of activation-energy asymptotics, analytical discussion was preoccupied with Damköhler-number asymptotics (i.e. $D \to 0$ or ∞). Knowledge of these limits is of some importance, so they will be briefly discussed first.

Frozen combustion occurs when the chemical reaction is very weak, i.e. $D \to 0$. The heat conducted back to the supply sphere then comes from the resevoir at infinity (provided $T_\infty > T_s$) and the limit solution is

$$T = (T_s - L) + Le^{M(1-1/r)} \tag{16}$$

where

$$M = M_w = \ell n \left[1 + (T_\infty - T_s)/L \right] \tag{17}$$

We shall only be concerned with conductive heat sinks, i.e. $L > 0$, so that

$$T_s < T_\infty \tag{18}$$

is required for Y to be positive; then M is also positive, as expected.

The result (16) is not uniformly valid since for large values of r the neglected reaction term decays more slowly than the transport terms. Defining

$$\varepsilon^2 = \tfrac{1}{2} D \, Z_\infty e^{-\theta/T_\infty} \tag{19}$$

leads to the expansion

$$T = T_\infty - \frac{\varepsilon M}{R} \left[T_\infty - T_s + L - 2(1-e^{-R}) \right] + o(\varepsilon) \tag{20}$$

for the coordinate $R = \varepsilon r$. The temperature gradient far from the supply is thereby corrected, so that the heat flow from the infinite reservoir can be

calculated as

$$\lim_{R\to\infty} \left(4\pi r^2 \frac{dT}{dr}\right) = 4\pi M(T_\infty - T_a). \tag{21}$$

When $T_a > T_\infty$ an O(1) amount of heat is supplied to the environment, which is usually the goal of combustion. The frozen limit is not an extinguished state, but rather one in which all the reaction takes place at essentially constant temperature far from the supply.

The equilibrium limits are obtained as $D \to \infty$. They are of great practical interest since even under standard atmospheric conditions many diffusion flames do have large Damköhler numbers. Clearly the limit $D\to\infty$ is singular, since the highest derivative in equation (15) is multiplied by a vanishingly small parameter D^{-1}. We may anticipate thin regions where the second derivative is very large and, when located in the interior of the combustion field, they are called Burke-Schumann flame sheets (Kassoy & Williams 1968). They should not be confused with the flame sheets that occur in activation-energy asymptotics. The thin regions can also be boundary layers but we shall look at the other, more common possibility first.

Outside the flame sheet the limit equation is simply

$$YZ = 0, \tag{22}$$

which represents chemical equilibrium for the irreversible reaction. The combustion field is divided into regions where either Y or Z vanishes. Since fuel is supplied at the sphere and oxidant at infinity it is natural to put an oxidant-free region contiguous with the sphere, separated at $r = r_*$ by a flame sheet from a fuel-free region extending to infinity. The Shvab-Zeldovich relations (12,13) then imply

(23) $$Z = 0,\ T = (T_s - L)(1 - e^{-M/r}) + (T_\infty + 2Z_\infty)e^{-M/r} \quad \text{for} \quad r < r_*,$$

(24) $$Y = 0,\ T = T_\infty + (T_a - T_\infty)(1 - e^{-M/r}) \quad \text{for} \quad r > r_*,$$

and the temperature at the sphere is T_s only if

(25) $$M = M_e = \ell n\left[1 + \frac{T_\infty - T_s + 2Z_\infty}{L}\right].$$

Continuity of temperature at the flame sheet shows that it must be located at

(26) $$r_* = M_e / \ell n\ (1 + Z_\infty),$$

so that the flame temperature is

(27) $$T_* = T_\infty + Z_\infty(T_a - T_\infty)(1 + Z_\infty).$$

These equations are the essence of the so-called Burke-Schumann solution, although it is still necessary to show that there is a structure linking the two sides of the flame sheet. We shall be content with setting up an apparently well-posed problem for this structure.

It is clear from the oxidant species equation (3b) that, for D large but not infinite, there can be no algebraic perturbation of $Z = 0$ in $r < r_*$. The temperature is therefore given to all orders by the formula (23) so that, on writing

(28) $$M = M_0 + D_*^{-1/3} M_1 + o(D_*^{-1/3}),\ M_0 = M_e,\ D_* = \tfrac{1}{2}De^{-\theta/T_*}$$

(a choice justified by the consistency of the structure problem below), we find

(29) $$T = T_0^- + D_*^{-1/3} M_1 (T_s - T_\infty - L - 2Z_\infty)e^{-M_0/r}/r^2 + o(D_*^{-1/3}).$$

where T_0^- is the original T in $r < r_*$ with M replaced by M_0. Similarly, there is no algebraic perturbation of Y in $r > r_*$ so that the temperature is

(31) $$T = T_0^+ + D^{-1/3} M_1 (T_a - T_\infty) e^{-M_0/r}/r + o(D_*^{-1/3}).$$

Within the flame sheet we set

(32) $$T = T_* + D_*^{-1/3} t + o(D_*^{-1/3}), \quad r = r_* + D_*^{-1/3}\xi$$

to obtain

(33) $$d^2t/d\xi^2 = -\frac{1}{4}\left[t + \left(\frac{T_a - T_\infty}{1+Z_\infty}\right)\left(\frac{M_0\xi}{r_*^2} - \frac{M_1}{r_*}\right)\right]\left[t + \left(\frac{T_a - T_\infty}{1+Z_\infty} - 2\right)\left(\frac{M_0\xi}{r_*^2} - \frac{M_1}{r_*}\right)\right].$$

Matching with the expansions outside requires that

(34) $$t = \left(\frac{T_\infty - T_a}{1+Z_\infty} + 2\right)\left(\frac{M_0\xi}{r_*^2} - \frac{M_1}{r_*}\right) + o(1) \quad \text{as} \quad \xi \to -\infty,$$

(35) $$\frac{dt}{d\xi} = \frac{T_\infty - T_a}{1+Z_\infty}\frac{M_0}{r_*^2} + o(1) \quad \text{as} \quad \xi \to +\infty.$$

It is reasonable to expect that, for some unique M_1 in the initial condition (34), integration of the structure equation (33) from $\xi = -\infty$ will lead to the correct slope (35) at $\xi = +\infty$. That indeed is found numerically, which is the only way of carrying out the integration. We may therefore assert that there is a structure and that its computation gives the perturbation of the burning rate.

The Burke-Schumann solution does not hold for all parameter values. An underlying assumption is that a flame sheet forms in the interior of the combustion field, so that for consistency r_* must be greater than 1, i.e.

(36) $$T_\infty - T_s > (L-2)Z_\infty .$$

Then M_0 is automatically positive, as might be expected. As equality is approached the flame sheet moves to the surface $r = 1$ and our analysis breaks down. Although the resulting surface flame (Buckmaster 1975) does not play as important a role in practice as the Burke-Schumann flame, a brief description of it will be given here.

When the flame sheet is a boundary layer the oxidant-free region is absent and only the fuel-free region (24) remains. Since the temperature must tend to T_s as $r \to 1$,

$$M = M_s = \ell n[1 + (T_\infty - T_s)/(L-2)] , \tag{37}$$

a result quite different from the Burke-Schumann value (25) but to which it is eqaul at the inequality (36). The result (37) is that for weak burning with L replaced by $L-2$, where the 2 can be identified as the heat released in the flame.

In addition, the flame-sheet structure is different. The Shvab-Zeldovich relation (13) shows that

$$Z_* = \frac{(T_s - T_\infty) - (2-L)Z_\infty}{T_\infty - T_a} \tag{38}$$

no longer vanishes. As a consequence the flame sheet now has thickness $D_*^{-1/2}$ and the structure is governed by a linear equation that can easily be integrated. We find

$$M = M_s [\, 1 + (D_* Y_{O*})^{-1/2} \frac{L(1+Z_\infty)}{(T_a - T_\infty)} + o(D_*^{-1/2})\,] \tag{39}$$

and the structure

$$T = T_s + D_*^{-1/2} M_O [\, \frac{T_\infty - T_a}{1+Z_\infty}\, \xi + \frac{L}{\sqrt{Z_*}} (1 - e^{-\sqrt{Z_*}\xi})\,] + o(D_*^{-1/2}), \tag{40}$$

where now $\xi = D_*^{1/2}(r-1)$.

Restrictions on the parameters comes from M_s and Z_*. The (small) mass fraction of fuel is positive only for $M_s > 0$, so that we must have

$$T_\infty \gtrless T_s \quad \text{according as} \quad L \lessgtr 2; \tag{41}$$

the positivity of Z_* imposes the additional restriction

(42) $$T_\infty - T_s \lessgtr (L-2)Z_\infty$$

Two angular regions are thereby determined in the parameter plane (Fig. 3); one coincides with the region where the Burke-Schumann solution exists but the weak-burning solution does not, and the other with the region where the reverse is true.

3. The Nearly Adiabatic Flame for $Le_i \neq 1$.

Having determined the possible ends of the M,D-response curve, we now turn to its shape in between. Here activation-energy asymptotics are particularly useful, though a general discussion is still quite complicated (see Law 1975) requiring extensive numerical calculations. For the moment we shall restrict attention to the special case considered by Buckmaster (1975) in which

(43) $$T_a - T_\infty = k/\theta \text{ as } \theta \to \infty ,$$

where $k = O(1)$. A great deal of qualitative insight into the nature of diffusion flames can thereby be obtained with a minimum of computations. The most important aspects of the general case will be dealt with later, albeit for $\theta \to \infty$ still.

It is convenient to fix everything but T_s such that its limiting value $T_\infty + L-2$ satisfies

(44) $$T_s < \min\{T_\infty, T_\infty + (2-L)Z_\infty\}$$

to ensure the existence of both the frozen and Burke-Schumann limits. Restriction to small values of $T_a - T_\infty$ means that in both limits the combustion field is nearly adiabatic, and in fact that will be true along the whole of the response curve. The unsteady formulation is reinstated, with Lewis numbers again arbitrary. Global Shvab-Zeldovich relations do not exist and it is necessary to re-examine the complete system (1-3).

For slow variations, the only information needed from such a system in Sec. II was the change in enthalpy $T + Y$ up to the flame sheet. Here the changes in both $T+2Y$ and $T+2Z$ are needed, but the procedure is the same except for integrating from the supply (as in Sec. IV$_s$) and taking account of the areal factor r^2. We find

$$M(T_a - T_* - 2Y_*) = \mathcal{J}(Y) - r_*^2\left(\frac{\partial T}{\partial r} + \frac{2}{\mathcal{L}}\frac{\partial Y}{\partial r}\right)_*, \tag{45}$$

$$M(T_a - 2 - T_* - 2Z_*) = \mathcal{J}(Z) - r_*^2\left(\frac{\partial T}{\partial r} + \frac{2}{m}\frac{\partial Z}{\partial r}\right)_*, \tag{46}$$

to $O(1/\theta)$, where

$$\theta\mathcal{J}(Y) \int_1^{r_*} r^2 \frac{\partial}{\partial \tau}[\rho(2Y - T_* - 2Y_*)]dr$$

is to be evaluated to $O(1)$ only; stars refer to values just behind the flame sheet. $\mathcal{J}(Z)$ will not be evaluated since the corresponding equation is only needed to $O(1)$.

So far as leading terms are concerned, we may concentrate on the steady version of equations (2), (3a) and (3b) where ρv is the function (10) with M now dependent on τ. Beyond the flame sheet the temperature must be constant at T_∞. Suppose, on the contrary, that it increases from the flame to infinity. Then heat from the infinite resevoir would maintain the flame temperature above $T_a = T_\infty$, which is a contradiction. The combustion field is therefore similar to that for the plane deflagration wave treated in Ch. II. The temperature increases from T_s at the supply to T_∞ at the flame, beyond which it stays constant. The reaction in $1 < r < r_*$ is frozen, while there is equilibrium with

$$Y = 0 \quad \text{in} \quad r_* < r < \infty. \tag{47}$$

In fact the latter holds to all orders.

With this picture in mind the solution in the frozen region is easily derived. We find

$$(48)\qquad T = T_s - L + Le^{M(1-1/r)} + o(1),\ Y = 1 - e^{\ell M(1/r_* - 1/r)} + o(1),\ Z = Z_* e^{m M(1/r_* - 1/r)} + o(1),$$

where

$$(49)\qquad r_* = M/(M + \ell n\ L/2).$$

These satisfy the supply conditions and give $T = T_\infty$ (to order 1), $Y = 0$ at $r = r_*$. For consistency r_* must be greater than 1, i.e.

$$L < 2$$

is required: the heat conducted back into the supply sphere must be less than that released in the flame. Similarly

$$(50)\qquad Z = [Z_*(1-e^{-Mm/r}) + Z_\infty(e^{-Mm/r} - e^{-Mm/r_*})]/(1-e^{-Mm/r_*}) + o(1),$$

$$(51)\qquad T = T_\infty + C(1-e^{-M/r})/\theta + o(1/\theta)$$

in the equilibrium region, because chemistry-free equations are still satisfied. (The constant T_∞ does not count as a leading term.) The unknown constants Z_* and C can be found (in terms of M) from the basic equations (45) and (46) of slow variations, which yield

$$(52)\qquad C = K - bM^2 dM/d\tau,\ Z_* = (1+Z_\infty)e^{-Mm/r_*} - 1$$

where

$$(53)\qquad b = \int_0^{\ell n(2/L)} \frac{2(Le^{\ell}/2)^{\ell} - Le^{\ell}}{T_s - L + Le^{\ell}} \frac{d}{d\ell}\left[\frac{\ell}{(\ell - M)^4}\right] d\ell\ .$$

The chemical reaction determines the burning rate at a given temperature, so that we may look to the structure of the flame sheet for another relation between M and the perturbation of the flame temperature, represented by C. Writing as usual

$$r = r_* + \xi/\theta \quad , \; T = T_\infty + t/\theta + o(1/\theta),$$

(54)

$$Y = y/\theta + o(1/\theta), Z = Z_* + z/\theta + o(1/\theta),$$

leads to the equations

$$-\partial^2 t/\partial\xi^2 = (2/\mathcal{L})\overbrace{\partial^2 y/\partial\xi^2} = \tilde{D} y \, e^{t/T_\infty^2}, \tag{55}$$

where

$$\tilde{D} = DZ_* \theta^{-2} e^{-\theta/T_\infty}, \tag{56}$$

while matching on either side of the flame gives the boundary conditions

$$t = 2M\xi/r_*^2 + O(1), \; y = -\mathcal{L}M\xi/r_*^2 + O(1) \quad \text{as } \xi \to -\infty, \tag{57}$$

$$t = C(1-e^{-M/r_*}) + o(1), \; y = o(1) \quad \text{as } \xi \to +\infty. \tag{58}$$

It follows that there is a local Shvab-Zeldovich relation

$$t + 2y/\mathcal{L} = C(1-e^{-M/r_*}), \tag{59}$$

which enables the equation for t to be integrated to give

$$C(1-e^{-M/r_*}) = T_\infty^2 \ln(2M^2\theta^2 e^{\theta/T_\infty}/D\mathcal{L}Z_* r_*^4 T_\infty^4). \tag{60}$$

Elimination of C between this and the result (52a) yields an equation for M, namely

$$(61) \qquad bM^2 dM/d\tau = k-(1-e^{-M/r_*})^{-1} T_\infty^2 \ell n(2M^2\theta^2 e^{\theta/T_\infty} \mathcal{D}\mathcal{L} Z_* r_*^4 T_\infty^4)$$

where Z_* and r_* are given by equations (52b) and (49).

We shall first describe the steady state, determined by setting the right-hand side of this last equation equal to zero, and then discuss its stability. Different values of k lead to different steady-state responses, i.e. curves of M versus D with all other parameters fixed (Fig. 4), though all join the frozen limit (17) to the Burke-Schumann limit (25). In between, a curve is monotonic or S-shaped depending on the value of k. When there is a gain of heat from infinity ($k<0$) or when the loss is sufficiently small, the response is monotonic. But for sufficiently large loss the burning rate is triple-valued over some range of Damköhler number. Conditions under which heat is provided to the environment are particularly important, so that the S-shaped response is of special interest.

Explicit formulas can be given for the turning points on the S when k is large. At the lower point

$$(62) \qquad M \sim \ell n(2/L) + 4T_\infty^2/k, \quad D \sim 2(4/e)^4 T_\infty^4 \theta^2 e^{\theta/T_\infty} (\ell n 2/L)^2 \mathcal{L} Z_\infty k^4,$$

while at the upper point

$$(63) \qquad M \sim M_e - T_\infty^2 L e^{M_e}/2k,$$

$$D \sim 4(M_e + \ell n\, L/2)^4 \theta^2 e^{\theta/T_\infty} k \exp\{-k[1-(1+Z_\infty)^{-m}]/T_\infty^2\} / L\mathcal{L} m M_e^2 T_\infty^6 e^{M_e},$$

where

$$(64) \qquad M_e = \frac{1}{m} \ell n(1 + Z_\infty) + \ell n(2/L)$$

is the Burke-Schumann value (25) corrected for $m \neq 1$.

Conclusions about the instability of the steady state can easily be drawn from the full equation (61), which holds in the strip $M_s < M < M_e$ where $Z_* > 0$ and $1 < r_* < \infty$. The right-hand side is positive to the right of the steady-state response curve and negative to the left (Fig. 5), while $b \gtrless 0$ according as $\mathcal{L} \lesseqgtr 1$. Consider first $\mathcal{L} < 1$. If the burning state lies off the steady-state curve, then M will change in the direction of the arrows in Fig. 5 so that the middle branch of the S is unstable. Now suppose $\mathcal{L} > 1$; the arrows must be reversed so that then the upper and lower branches of the S, and the whole of the monotonic curve, are seen to be unstable.

Nothing may be concluded about stability however, since only a special class of disturbances is being considered. Indeed, it is generally believed that the middle branch of the S, which is stable to the present disturbances, is in fact unstable. Whether that is true or not, certainly the top and bottom branches are more important than the middle branch because for sufficiently large and small values of D they represent the only possible steady states. The instability predicted for $\mathcal{L} > 1$ is therefore the most interesting result, and it is analogous to the instability of the premixed plane flame (Ch. II) to one-dimensional disturbances when the Lewis number is greater than one. Plane flames are also unstable when the Lewis number is less than one if three-dimensional disturbances whose wavelengths are large compared to the flame thickness are permitted (Ch. V), but this result clearly has no analog for a spherical flame.

If it is assumed that the stability results deduced here for $\mathcal{L} < 1$ are generally true, i.e. when all possible disturbances are accounted for, the middle branch is unstable and the other two are stable, then the turning points of the S are ignition and extinction points. The asymptotic results (62) and (63) then give ignition and extinction conditions, respectively. In any event, there is no reason to doubt their validity for $\mathcal{L} = 1$.

4. General Ignition and Extinction Analyses with $\mathcal{L} = m = 1$.

We proceed now to the general steady state, i.e. arbitrary values of $T_a - T_\infty$, with emphasis on the top and bottom branches of S-responses. As in Sec. 2 the qualitative nature of the solution is not affected by the Lewis numbers so that, since the analysis is complicated enough for $\mathcal{L} = m = 1$, we shall restrict attention to these values; there is anyway a lack of stability for $\mathcal{L} > 1$ and some question of it for $\mathcal{L} < 1$, at least for T_∞ close to T_a (Sec. 3).

We have to deal with the Shvab-Zeldovich relations (12), (13) and the temperature equation (15). The requirement (44) is still imposed, for the same reason. The additional requirement

(65) $$T_\infty < T_a$$

ensures an S-response, as is suggested by Sec. 3 where such a response was only obtained for sufficiently large $k = \theta(T_a - T_\infty) > 0$. [When T_∞ is less than T_a, the second part of the original requirement (44) is actually implied by the first.]

The lower branch will be considered first, the main goal being to locate the ignition point, which is a fundamental characteristic of the burning response. Sec. 3 suggests that the burning will take place far from the supply on the whole lower branch, i.e. with M close to its frozen value: the ignition point (62) has this property, albeit the measure of closeness is $1/k$ rather than the $1/\theta$ we must expect now.

At any finite value of r the combustion field is frozen to all orders, so we may write

(66) $$T = T_s - L + Le^{M_w(1-1/r)} + \theta^{-1} M_1 L(1-1/r) e^{M_w(1-1/r)} + o(\theta^{-1})$$

where

(67) $$M = M_w + \theta^{-1} M_1 + o(\theta^{-1}).$$

T and T' take the correct values at $r = 1$ but the condition $T \to T_\infty$ as $r \to \infty$ is violated, showing that a new coordinate is required there. It turns out to be

$$R = r/\theta \tag{68}$$

and then the expansion

$$T = T_\infty + \theta^{-1} t(R) + o(\theta^{-1}) \tag{69}$$

leads to the structure equation

$$\frac{1}{R^2}\frac{d}{dR}\left(R^2 \frac{dt}{dR}\right) = D_w \left[t - \frac{(T_a - T_\infty)M_w}{R}\right] e^{t/T_\infty^2}, \quad D_w = DZ_\infty \theta^{-2} e^{-\theta/T_\infty/2} \tag{70}$$

subject to the boundary conditions

$$t = Le^{M_w}(M_1 - M_w/R) + o(1) \quad \text{as} \quad R \to 0, \quad t = o(1) \quad \text{as} \quad R \to \infty, \tag{71}$$

the first of which comes from matching with the frozen expansion. With all parameters specified, including D_w the perturbation t can be found (numerically) without using the M_1-term. In that way M_1 can be determined as a function of the Damköhler number.

By suitably scaling D_w and M_1 the relation between them can be made to depend on a single paramter

$$\beta = (T_a - T_\infty)/Le^{M_w}. \tag{72}$$

The scaling is

$$\Delta_w = \alpha^2 D_w, \quad N_w = \alpha M_1/M_w \quad \text{where} \quad \alpha = M_w Le^{M_w}/T_\infty^2, \tag{73}$$

and then the new variables

$$u = \rho t/T_\infty^2, \quad \rho = R/\alpha \tag{74}$$

lead to the canonical problem

(75) $$d^2u/d\rho^2 = \Delta_w(u-\beta)e^{u/\rho},$$

(76) $$u = N_w\rho - 1 + o(1) \quad \text{as} \quad \rho \to 0, \quad u = o(1) \quad \text{as} \quad \rho \to \infty$$

It is found, albeit numerically, that the graphs of N_w versus Δ_w display the ignition phenomenon if and only if β is positive. Curves for various values of β are shown in Fig. 6; note that they are independent of Z_∞.

The burning rate at the extinction point (63) of the nearly adiabatic flame lies close to the Burke-Schumann value when k is large. This suggests that the general extinction curve can also be uncovered by an analysis which considers $O(\theta^{-1})$ perturbations of the burning rate, now from its Burke-Schumann value.

The flame sheet has the location (26) while on both sides of it the reaction is frozen to all orders. Thus

(77) $$T = \begin{cases} T^- = T_S - L + Le^{M_e(1-1/r)} + \theta^{-1}M_1L(1-1/r)\, e^{M_e(1-1/r)} + o(\theta^{-1}) & \text{for } r < r_*, \\ T^+ = T_a + (T_\infty - T_a)e^{-M_e/r} + o(1) & \text{for } r > r_*, \end{cases}$$

where

(78) $$M = M_e + \theta^{-1}M_1 + o(\theta^{-1}).$$

Only M_1 is unknown and for that we must turn to the structure of the flame sheet. With

(79) $$r = r_* + \xi/\theta$$

the expansion

(80) $$T = T_* + \theta^{-1}t(\xi) + o(\theta^{-1}),$$

where T_* is the flame temperature (27), leads to the structure equation

$$(81)\quad \frac{d^2t}{d\xi^2} = -D_e\Big[t+\Big(\frac{T_a-T_\infty}{1+Z_\infty}\Big)\Big(\frac{M_e\xi}{r_*^2}-\frac{M_1}{r_*}\Big)\Big]\Big[t+\Big(\frac{T_a-T_\infty}{1+Z_\infty}-2\Big)\Big(\frac{M_e\xi}{r_*^2}-\frac{M_1}{r_*}\Big)\Big]e^{t/T_*^2},\quad D_e = D\theta^{-3}e^{-\theta/T_*}$$

subject to the boundary conditions

$$t = \Big(2-\frac{T_a-T_\infty}{1+Z_\infty}\Big)\Big[\frac{M_e\xi}{r_*^2}+\Big(1-\frac{1}{r_*}\Big)M_1\Big]+o(1)\quad \text{as } \xi\to-\infty,$$

$$(82)$$

$$\frac{dt}{d\xi} = -\Big(\frac{T_a-T_\infty}{1+Z_\infty}\Big)\frac{M_e}{r_*^2}+o(1)\quad \text{as } \xi\to+\infty,$$

which comes from matching. This should be compared with the problem (33), (34) and (35), the only difference being that here the Arrhenius factor is not approximated by a constant since the perturbations are as large as $O(\theta^{-1})$.

Again the problem determines M_1 and, by suitable scaling, the relation between it and D_e can be made to depend on the single parameter

$$(83)\qquad \gamma = 1-(T_a-T_\infty)/(1+Z_\infty) = 1-\beta\ .$$

Then

$$(84)\qquad \Delta_e = r_*^4T_*^6D_e/M_e^2,\quad N_e = (1+\gamma)M_1/T_*^2,$$

and

$$(85)\qquad u = t/T_*^2-\gamma\rho\ ,\quad \rho = (M_e\xi/r_*^2-M_1/r_*)/T_*^2$$

leads to the canonical problem

$$(86)\qquad d^2u/d\rho^2 = -\Delta_e(u^2-\rho^2)\exp(u+\gamma\rho),$$

$$(87)\qquad u = \rho+N_e+o(1)\quad \text{as } \rho\to-\infty\ ,\ du/d\rho = -1+o(1)\quad \text{as } \rho\to+\infty\ .$$

It is found (though again numerically) that the graphs of N_e versus Δ_e display the extinction phenomenon if and only if γ is less than 1, i.e. $\beta = 1-\gamma$ is positive. Curves for various values of γ are shown in Fig. 7. Note that the actual Damköhler number for extinction is $O(\theta^3e^{\theta/T_*})$ as compared to $O(\theta^2e^{\theta/T_\infty})$ for ignition, so that (since $T_* > T_\infty$) the extinction point lies to the left of the ignition point, as it should.

5. Remarks on the Middle Branch.

It is widely believed that the middle branch, where M is a decreasing function of D, is not of practical interest because the burning states there are unstable. However, there is no hard theoretical evidence for this other than the slow-time instability for $\mathcal{L} < 1$ described in Sec. 3. Certainly the notion that for a laboratory flame an increase in pressure could cause a decrease in burning rate is intuitively difficult to accept but, be that as it may, there are at least two good reasons for studying the middle branch. Any definitive answer to the stability question can surely come only after the nature of the steady state has been determined; and anyway that nature is sufficiently different from what we have encountered before that some account of it should be given. Nevertheless, only a broad sketch will be presented.

It is clear from the ignition and extinction analyses that the flame temperature on the middle branch must span the range T_∞ to $T_\infty + Z_\infty(T_a - T_\infty)/(1+Z_\infty)$ and, since it is the maximum temperature at both ends, we may expect it to be so in between. On either side of the flame sheet the reaction is frozen, just as in the extinction analysis. The key difference is that here Y_* and Z_* do not both vanish; we shall first suppose that neither does.

It is more convenient now to specify M and determine

$$D = D_0[1 + O(\theta^{-1})] \tag{88}$$

as part of the solution. The expansions (77) are therefore replaced by

$$T = \begin{cases} T^- = T_s - L + Le^{M(1-1/r)} + o(1) & \text{for } r < r_*, \\ T^+ = T_\infty + Le^{M}(1-e^{-M/r}) + o(1) & \text{for } r > r_*, \end{cases} \tag{89}$$

if we anticipate a property of the flame structure, namely that the heat generated by the reaction is conducted equally to the two sides. Continuity of temperature to leading order at the flame sheet now determines

$$r_* = M/\ell n\ 2/(1+e^{M_w-M}) \tag{90}$$

and

$$T_* = (T_s+T_\infty-L+Le^M)/2, \tag{91}$$

which covers its range as M increases from M_w to M_e.

The sturcture is investigated, in the usual way, by means of the transformation (79) and the expansion (80) and we find

$$\frac{d^2t}{d\xi^2} = -D_m e^{t/T_*^2},\quad D_m = D_O Y_* Z_* \theta^{-1} e^{-\theta/T_*} \tag{92}$$

where Y_* and Z_* are determined by the Shvab-Zeldovich relations (12) and (13). Integration yields

$$(\frac{dt}{d\xi})^2 = C - 2D_m T_*^2 e^{t/T_*^2}, \tag{93}$$

where C is a constant; from which it follows that the temperature gradients on the two sides of the flame sheet are of equal magnitude but of opposite sign, as anticipated earlier. [Matching shows that $C = (Le^M M/r_*^2)\exp(-M/r_*)$, but we shall not need this result.]

Another integration gives only a relation between the maximum value of t and its location; to determine D_m it is necessary to take the expansion (80) to one more term. No useful purpose is served by presenting these rather complicated algebraic details. They are described by Liñán (1974) for the counterflow flame and Law (1975) has adapted Liñán's analysis to the present problem. Another reason for not pursuing the determination of D_m is that

(94) $\ell n D_0 = \theta/T_* + \ell n\,\theta + \ell n(D_m/Y_* Z_*)$

is only affected to $O(1)$ by it, T_* being a known function (91) of M. Indeed the expected property

$$dD_0/dM < 0 \quad \text{as} \quad \theta \to \infty$$

follows, irrespective of the value of D_m, since

(95) $$dT_*/dM > 0.$$

The solution derived here is valid only so long as $0 < Y_*, Z_* < 1$ and $r_* > 1$. These inequalities are satisfied automatically with the exception of $Y_{F*} > 0$, which requires

(96) $$M < \ell n(T_a - T_\infty)/L.$$

Since M must be greater than M_w the condition for there to be a range of validity is

(97) $$T_\infty < T_a - 1;$$

the range will extend up to M_e if

(98) $$T_\infty < T_a - (1+Z_\infty).$$

These possibilities are shown in Fig. 3.

When this last condition is not satisfied, a question arises of completing the range $M_w < M < M_e$. The clue is the vanishing of Y_* at the end of the range: for the remaining values of M (and all of them when $T_a - T_\infty < 1$) the mass fraction of fuel is $O(\theta^{-1})$ at the flame sheet. This leads to a similar analysis, albeit with a different flame structure (cf. Sec. 6), which completes the middle branch. On it Z_* decreases from Z_∞ at one end to zero at the other so as to join the

ignition and extinction branches. In that connection it should be noted that the middle branch does not join directly to the extinction branch when the original solution completes it. Although Z_* vanishes at M_e, Y_* does not; so that a transition flame, for which Y_* decreases to zero, is needed. All these details are described by Liñán (1974) for the counterflow problem.

6. The Monotonic and Other Responses.

The last two sections have been concerned with the S-shaped response which occurs when the combustion field supplies heat to the ambient atmosphere. When

(99) $$T_\infty > T_a$$

the flux is in the opposite direction and we may expect the response to be monotonic (if only on the basis of Sec. 3). Fuel drops, to which the theory will be adapted in Sec. 8, are usually burnt to provide heat to their surroundings so that from the point of view of that precise application the present discussion is not important.

The temperature increases again beyond the flame sheet to give an equilibrium region, where

(100) $$Y = 0 \quad \text{for} \quad r > r_*$$

must hold to all orders. It follows that the expression (89a) is still correct, but that the expansion (89b) must be replaced by the asymptotically exact result

(101) $$T = T^+ = T_\infty + (T_a - T_\infty)(1 - e^{-M/r}) \quad \text{for} \quad r > r_*.$$

Continuity at the flame sheet then determines

(102)
$$r_* = M/\ell n\,[(T_a - T_\infty + Le^M)/2\,]$$

$$T_* = T_a + 2(T_\infty - T_a)/(Le^M - T_\infty + T_a).$$

The monotonicity of the response is now clear without going into details of the structure, by extracting just

$$\ell n\, D_0 = \theta/T_* + 2\, \ell n\theta + O(1) \tag{103}$$

in analogy with the expansion (36). Since

$$dT_*/dM < 0 \tag{104}$$

under the condition (99), the leading term D_0 in the Damköhler number is an increasing function as required.

As M increases from its frozen value, r_* decreases from ∞ and there are two possibilities. If the inequality (36) is satisfied (see Fig. 3), r_* reaches the value (26) as M tends to M_e; the combustion field is then identical to the Burke-Schumann, in particular the oxidant no longer penetrates through the flame. Our solution joins the frozen limit to the Burke-Schumann limit, correct descriptions of the approaches to which follow the same lines as Sec. 4.

The second possibility arises when

$$0 < T_\infty - T_s < (L-2)Z_\infty \tag{105}$$

(see Fig. 3). Then M_s is smaller than M_e and as M reaches it the flame settles down on the surface of the supply sphere. Our solution now joins the frozen limit to Buckmaster's limit, though we shall not describe the approaches here.

The discussion so far in this section can be justified by the fuel drop, albeit under conditions of little practical interest. The same is true for

$$T_\infty < T_s, \tag{106}$$

though the inequality can no longer hold over the whole response of the drop (see the next section). For this reason, no analysis for the lower half of Fig. 3 has been published although it is not difficult to see how it would go.

While there is no frozen limit now, it turns out that both equilibrium limits exist, provided

(107) $$T_\infty - T_s > (L-2)Z_\infty .$$

Otherwise, no limits exist and we must conclude that there is no solution. Indeed, application of the Shvab-Zeldovich relations (12) and (13) at $r = 1$ shows that the fuel and oxidant fractions there would be negative for $L > 2$ and for $T_\infty - T_a < -2(1+Z_\infty)$, respectively, even for finite θ, which leaves only a small triangle of doubt.

It is reasonable to suppose that, when the conditions (106) and (107) are satisfied, the response takes the form of a C joining Buckmaster's limit to the Burke-Schumann limit (which is always higher). Indeed, the analysis sketched in Sec. 5 will still apply; only the conditions under which the basic solution must be modified will change: $r_* > 1$ is no longer automatic and the basic solution applies over at least part of the range $M_s < M < M_e$ only when $L < 1$.

The leftmost point of the C-shaped curve represents both ignition and extinction conditions. Since the response determined by Sec. 5 has negative slope, the burning rate there will again lie within $O(1/\theta)$ of the Burke-Schumann value M_e. Hence the extinction analysis of Sec. 4 locates these conditions.

7. The Burning Fuel Drop.

In our discussion of the spherical diffusion flame we have supposed the seven parameters

$$T_s, L, J_s, K_s, T_\infty, Y_\infty, Z_\infty$$

to be given; indeed, we have taken

$$J_s = 1,\ K_s = 0,\ Y_\infty = 0$$

for simplicity. If L is the latent heat of the vaporization of the fuel (taken to be constant for the temperature range of interest), then these are in fact prescribed in fuel-drop burning with the exception of T_s, in place of which the Clausius-Clapeyron relation

$$Y_s = (T_s/T_b)^{\beta} \exp \hat{\theta}(1/T_b - 1/T_s) \tag{108}$$

is substituted. Here T_b is the boiling temperature corresponding to p_c i.e., in the notation of equation (III.16),

$$T_b^{\beta} \exp(-\hat{\theta}/T_b) = p_c/k. \tag{109}$$

Now Y_s may be calculated in terms of the existing parameters and M by means of the Shvab-Zeldovich relation (12), so that it may be eliminated to give

$$2(T_s/T_b)^{\beta} \exp \hat{\theta}(1/T_b - 1/T_s) = 2-L+(T_\infty - T_s + L - 2)e^{-M} \tag{110}$$

as the equation determining T_s. The new feature therefore is that T_s is no longer fixed but must be calculated at each point of the response curve. Once T_s is found, the parameter plane of Fig. 3 may be used to find the appropriate structure for determining D.

The properties of the resulting responses are not obvious and it helps to characterize the loci in the parameter plane. First note that there is always a weak burning limit, whatever the values of $L, T_\infty, Z_\infty, \hat{\theta}$ and T_b. That is, the equation (110) invariably has a solution $T_s = T_w$ (say) when M is set equal to M_w; in fact, $T_w < T_\infty$ as we should expect in the absence of weak burning for $T_s > T_\infty$. Next note that there is always a Burke-Schumann limit $T_s = T_e$ (say) when

$$T_\infty > (L-2)Z_\infty; \tag{111}$$

that $T_e < T_\infty + (2-L)Z_\infty$, corresponding to a point above the quilibria divider; and that $T_e \lesseqgtr T_w$ according as the point is above or below the adiabatic line. These results follow on setting $M = M_e$ in equation (110). Finally note that, when $M = M_s$, the equation has the solution $T_s = 0$. While this is not relevant when the inequality (44) holds, it provides a termination point when

(112) $$T_\infty < (L-2)Z_\infty.$$

The possible loci are illustrated in Fig. 8, where dashes indicate that the corresponding lines may or may not be crossed (depending on T_b and $\hat{\theta}$). The arrows show the direction of increasing M and follow from the property

(113) $$dT_s/dM \gtreqless 0 \text{ according as } T_s \gtreqless T_\infty + L - 2$$

of equation (110). [The condition $T_s \leq T_b$, i.e. $Y_s \leq 1$, is always satisfied.] Our knowledge of the response curves for fixed points in the paramter plane now suggests that the location of the point w determines whether the fuel-drop response is S-shaped or monotonic. Proof lies in the inequalities (95) & (104), which continue to hold when T_s varies with M according to the equation (110).

In short, qualitative results for fuel-drop burning can be deduced from the analysis of general spherical flames given in previous sections. However, quantitative results such as the graphs in Figs. 6 & 7 cannot be carried over: the variations of T_s, while they are only $O(1/\theta)$ on the upper and lower branches, will modify the ignition and extinction values (Ludford & Normandia 1978).

These remarks apply to steady burning; the unsteady analysis of Sec. 3 is not directly applicable since no account is taken of conditions in the interior of the drop. Some of the heat flux at the surface now accounts for changes in the interior temperature, so that there is a connection between it and the surface

temperature. As a consequence, L is the sum of the latent heat of vaporization and a complicated integral term depending on T_s. Such difficulties do not arise for the counterflow flame, but there the serious compromises with the fluid mechanics which are necessary cast doubt on the results.

References

Buckmaster, J.D. 1975, A new large Damköhler number theory of fuel droplet burning, Combustion and Flame 24, 79-88.

Buckmaster, J.D. 1975, Combustion of a liquid fuel drop, Letters Appl. Eng. Sci 3, 365-372.

Kassoy, D.R. and Williams, F.A. 1968, Effects of chemical kinetics on near equilibrium combustion in nonpremixed systems, Phys. Fluids 11, 1343-1351.

Law, C.K. 1975, Asymptotic theory for ignition and extinction in droplet burning, Comb. Flame 24, 89-98.

Liñán, A. 1974, The asymptotic structure of counterflow diffusion for large activation energy, Acta Astronautica 1, 1007-1039.

Matalon, M., Ludford, G.S.S. and Buckmaster, J. 1978, Diffusion flames in a chamber, to appear in Acta Astr.

Williams, F.A. 1965, Combustion Theory, Reading Massachusetts: Addison-Wesley.

Figures.

1. Counterflow diffusion flame
2. Fuel drop diffusion flame.
3. Paramter plane.
4. Near-adiabatic response curves.
5. Stability for near-adiabaticity.
6. Δ_w versus N_w.
7. Δ_e versus N_e.
8. Loci of T_s for fuel drop.

Fig. 3 (Ch. VI)

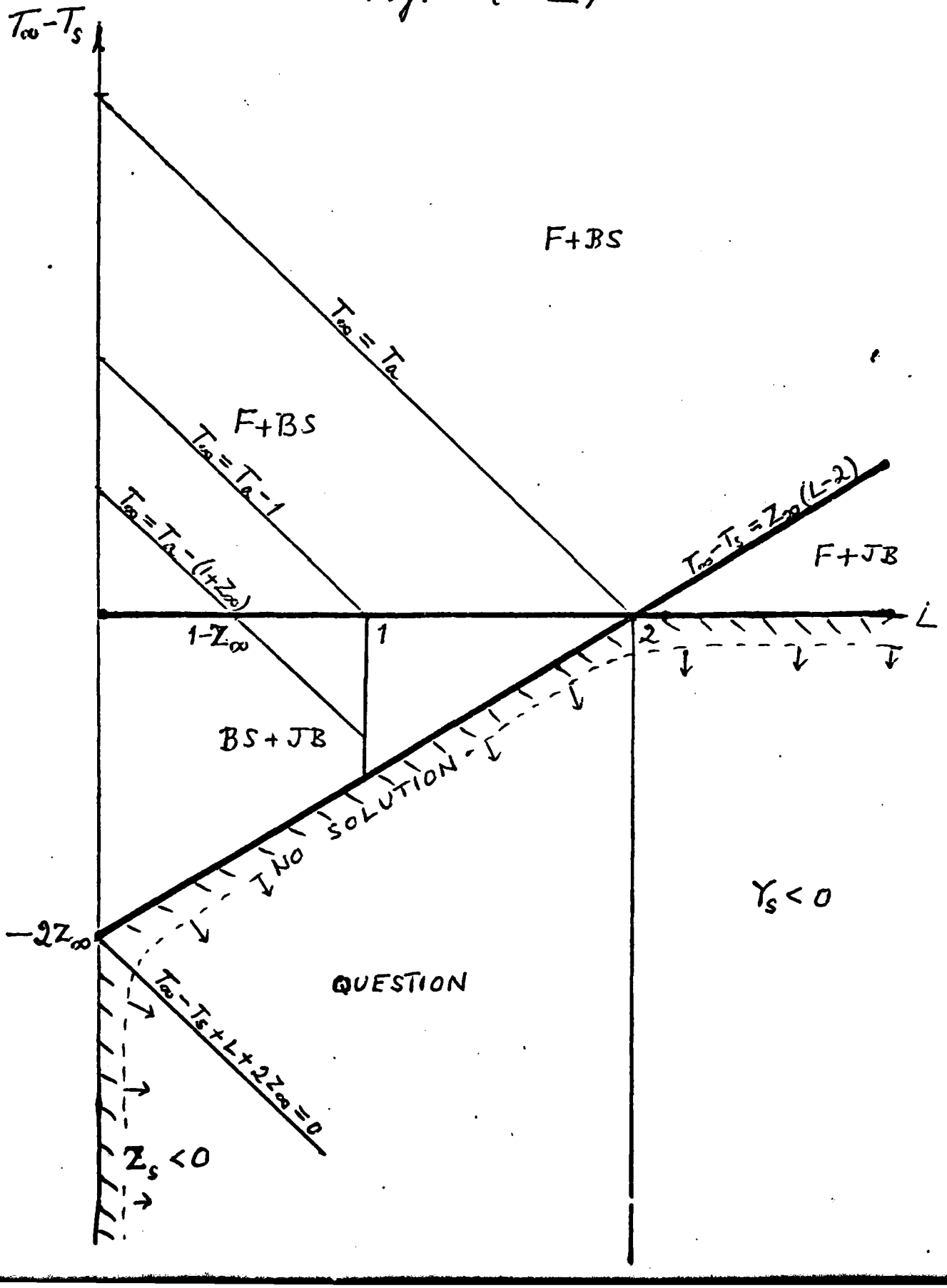
$T_\infty - T_s$
F+BS
$T_\infty = T_a$
F+BS
$T_\infty = T_a - 1$
$T_\infty = T_a - (1+Z_\infty)$
$T_\infty - T_s = Z_\infty (L-2)$
F+JB
$1-Z_\infty$
1
2
L
BS+JB
NO SOLUTION
$-2Z_\infty$
$Y_s < 0$
QUESTION
$T_\infty - T_s + L + 2Z_\infty = 0$
$Z_s < 0$

UNCLASSIFIED

SECURITY CLASSIFICATION OF THIS PAGE (When Data Entered)

REPORT DOCUMENTATION PAGE	READ INSTRUCTIONS BEFORE COMPLETING FORM
1. REPORT NUMBER: 108	2. GOVT ACCESSION NO.: AD-A084 430
	3. RECIPIENT'S CATALOG NUMBER:
4. TITLE (and Subtitle): MATHEMATICAL THEORY OF LAMINAR COMBUSTION VI: Spherical Diffusion Flames	5. TYPE OF REPORT & PERIOD COVERED: Interim Technical Report
	6. PERFORMING ORG. REPORT NUMBER:
7. AUTHOR(s): J.D. Buckmaster & G.S.S. Ludford	8. CONTRACT OR GRANT NUMBER(s): DAAG29-79-C-0121
9. PERFORMING ORGANIZATION NAME AND ADDRESS: Dept. of Theoretical and Applied Mechanics, Cornell University, Ithaca, NY 14853	10. PROGRAM ELEMENT, PROJECT, TASK AREA & WORK UNIT NUMBERS: P-15882-M
11. CONTROLLING OFFICE NAME AND ADDRESS: U. S. Army Research Office, Post Office Box 12211, Research Triangle Park, NC 27709	12. REPORT DATE: March 1980
	13. NUMBER OF PAGES: 30
14. MONITORING AGENCY NAME & ADDRESS (if different from Controlling Office)	15. SECURITY CLASS. (of this report): Unclassified
	15a. DECLASSIFICATION/DOWNGRADING SCHEDULE: NA

16. DISTRIBUTION STATEMENT (of this Report)

Approved for public release; distribution unlimited.

17. DISTRIBUTION STATEMENT (of the abstract entered in Block 20, if different from Report)

NA

18. SUPPLEMENTARY NOTES

The findings in this report are not to be construed as an official Department of the Army position, unless so designated by other authorized documents.

19. KEY WORDS (Continue on reverse side if necessary and identify by block number)

Spherical diffusion flames, Damköhler-number asymptotics, nearly adiabatic, ignition and extenction, S-response, C-response, monotonic response, fuel drop.

20. ABSTRACT (Continue on reverse side if necessary and identify by block number)

This report is Chapter VI of the twelve in a forthcoming research monograph on the mathematical theory of laminar combustion. Spherical diffusion flames are discussed with a view to application to the burning fuel drop. Emphasis is on establishing ignition and extinction conditions.

DD FORM 1 JAN 73 1473 EDITION OF 1 NOV 65 IS OBSOLETE

Unclassified

SECURITY CLASSIFICATION OF THIS PAGE (When Data Entered)